Abstract

Gain stability has long been identified as a key attribute for successful long-term operation of both space and terrestrial helix traveling wave tubes (TWTs), whose mission life may extend to 15 or more years. Gain change associated with attenuator (carbon) thin film resistivity change has been observed for at least 30 years; however no definitive experimental evidence to support the various resistance change theories has been available. Using a modified ion source, changes in film resistivity caused by low energy hydrogen ion bombardment of the carbon attenuator have now been positively identified as the cause of gain growth in helix TWTs. Carbon films experimentally damaged by ion bombardment compare identically to those removed from TWTs with thousands of operating hours. An unusual thermal annealing effect seen in TWT films has also been duplicated. Two potential methods to mitigate gain change have also been proposed based on this work.

Introduction

Gain change is a phenomenon that can occur in traveling wave tubes resulting in a change over time in a traveling wave tube's (TWT's) RF output level. Although a modest effect (typically less than 2 dB in amplifiers with greater than 50 dB of gain) it can be troublesome for amplifier systems because changing gain levels can result in uncompensated power changes or require added system complexity by requiring the incorporation of RF input level control. A typical example of gain change over life in a TWT is shown in Fig. 1. The gain starts out changing quickly and then changes more slowly as the TWT ages. For some TWTs, the rate of change may go to zero. For others, a small, linear rate of change lasts for the life of the TWT.

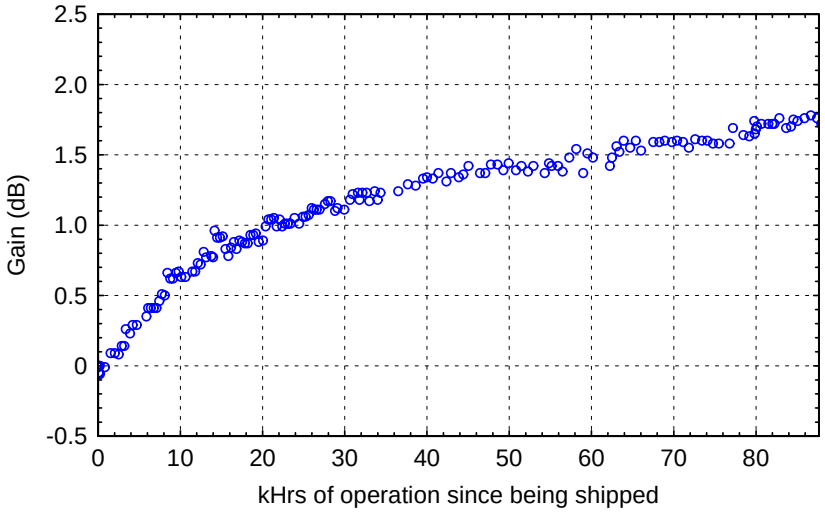

Fig 1. Measured gain change over the operational life of a helix TWT.

Gain change has been investigated for over 30 years, typically by disassembling and evaluating TWTs that have operated for thousands of hours. Although the cause of gain change has been positively identified as being due to changes in the resistivity of the

Report Documentation Page

Form Approved
OMB No. 0704-0188

1. REPORT DATE	2. REPORT TYPE	3. DATES COVERED
01 FEB 2007	**N/A**	**-**

4. TITLE AND SUBTITLE	5a. CONTRACT NUMBER
Congressional-Microwave Vacuum Electronics Power Res. Ini.) TWT Coatings Improvement Investigation	5b. GRANT NUMBER
	5c. PROGRAM ELEMENT NUMBER
6. AUTHOR(S)	5d. PROJECT NUMBER
	5e. TASK NUMBER
	5f. WORK UNIT NUMBER
7. PERFORMING ORGANIZATION NAME(S) AND ADDRESS(ES) **L-3 Communications-Electron Technologies 3100 W. Lomita Blvd Torrance, CA 90505-5510**	8. PERFORMING ORGANIZATION REPORT NUMBER
9. SPONSORING/MONITORING AGENCY NAME(S) AND ADDRESS(ES)	10. SPONSOR/MONITOR'S ACRONYM(S)
	11. SPONSOR/MONITOR'S REPORT NUMBER(S)

12. DISTRIBUTION/AVAILABILITY STATEMENT
Approved for public release, distribution unlimited

13. SUPPLEMENTARY NOTES
The original document contains color images.

14. ABSTRACT

15. SUBJECT TERMS

16. SECURITY CLASSIFICATION OF:			17. LIMITATION OF ABSTRACT	18. NUMBER OF PAGES	19a. NAME OF RESPONSIBLE PERSON
a. REPORT	b. ABSTRACT	c. THIS PAGE			
unclassified	**unclassified**	**unclassified**	**SAR**	**24**	

attenuator film, and detailed hypotheses exist regarding mechanisms that could cause these physical changes, no experimental verification of gain change hypotheses have previously been successful. Attenuator films removed from TWTs indicate that when the TWT gain has increased during its operational life, a corresponding overall increase in the resistivity of the attenuator has occurred. This is the most typical scenario; however gain decreases are also possible.

Basic Operation Principals of a Helix TWT

The helix TWT is a microwave amplifier that relies on the interaction of an electron beam with a low-level microwave signal. The microwave signal modulates the electron beam, redistributing the beam electrons into bunches. The electron bunches in turn transfer kinetic energy into the signal, resulting in amplification or gain. This effect occurs over many helix "turns" hence TWTs are often called "distributed" amplifiers. TWTs with amplification ratios approaching 60 dB are quite common.

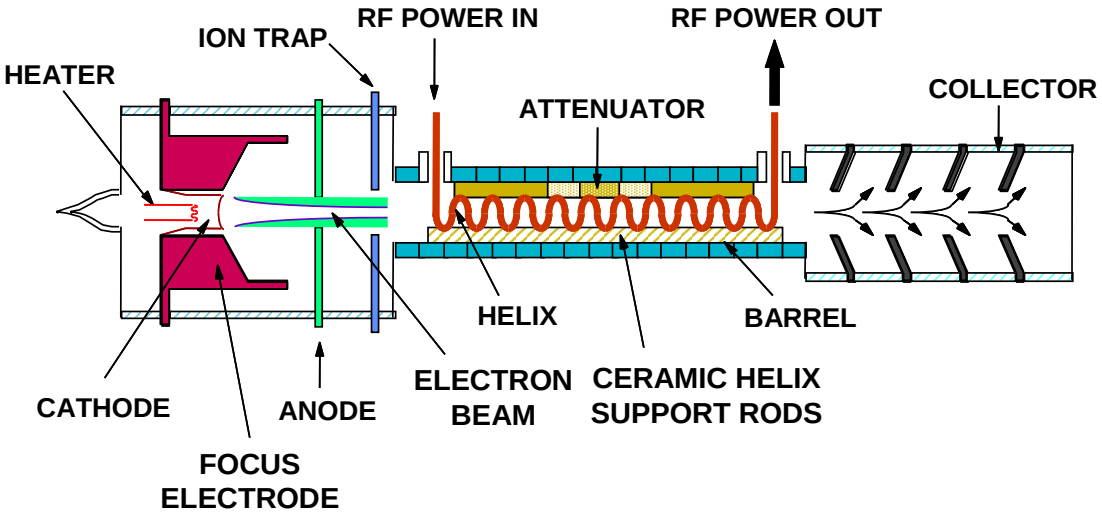

Fig. 2. Schematic model of a typical helix traveling wave tube.

A modern TWT (Fig. 2) is an ultra-high vacuum (UHV) device that includes an electron source (cathode), electron beam forming optics (electron gun), a magnetic electron beam transport system (magnetic structure), microwave input and output ports (windows), a slow-wave structure (SWS) which interacts with the electron beam to provide the RF amplification, and a beam collection system (collector). For a helix TWT, the SWS is a helix typically supported by three dielectric supports ("rods"). Although referred to as "tubes,," a modern TWT vacuum envelope is constructed of metal and ceramic, and does not contain glass.

Although not a new technology, continuous improvements have resulted in TWTs that can exceed 70% electrical efficiency, display octave or greater bandwidth or provide continuous output power of several kilowatts. TWTs are generally applicable in the

microwave frequency band from 500 MHz to over 40 GHz. Although TWTs contain relatively few parts, they depend on a unique and complex balance of carefully selected dielectric and metallic materials, thin films and extremely clean surfaces. These careful material selections and manufacturing processes result in a device that can operate reliably for hundreds of thousands of hours.

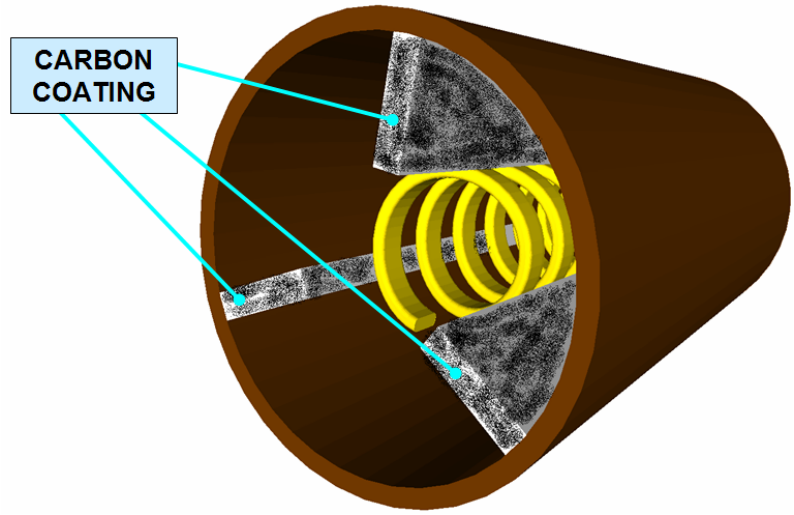

Fig. 3. Cross section of the inside of a helix TWT where the lossy coating is shown on the dielectric support rods.

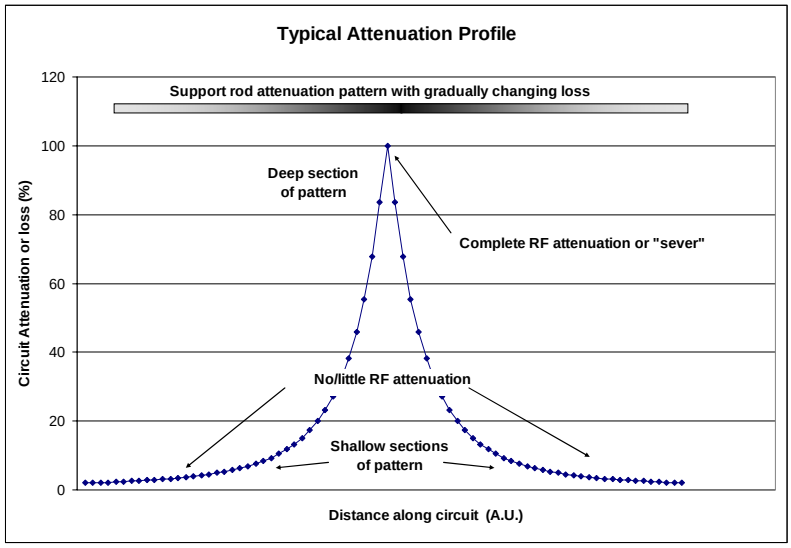

Fig. 4. Profile of attenuation pattern on a TWT helix support rod.

The TWT Attenuator

In a helix TWT it is desirable to separate the circuit into two parts: an input section that modulates the electron beam, and an output section that transfers beam kinetic energy into microwave energy[1]. A convenient method of performing this separation is to apply a

resistive thin film to the dielectric support rods that support the helix in the vacuum envelope (Fig. 3). The resistance profile of this thin-film helix "sever" controls the TWT gain and isolates the input and output ports by absorbing mismatch reflections within the TWT. To minimize step discontinuities in transmission line impedance, the thin film is patterned such that the resistive loss or "attenuation" starts out slowly and gradually transitions to higher levels (Fig. 4). Loss patterning is achieved by varying the film thickness. Carbon thin films are typically used for attenuation because the bulk resistivity of carbon allows for films which have reasonable thickness (0.1-10 μm). Carbon films are also easily applied by sputter coating or the thermal decomposition of hydrocarbon molecules[2].

Previous Gain Stability Investigations

Because the attenuation profile affects the beam-wave interaction in a TWT, the (resistive) stability of the attenuator thin film directly impacts TWT performance, typically resulting in the TWT gain increasing over time. Gain changes associated with attenuator resistivity changes have been observed and investigated by several authors. Behler[3] surveyed attenuators removed from TWTs with from 1,200 to over 70,000 hours of operation, making the first known connection between gain change and attenuator film degradation. Resistivity changes were more pronounced in thicker films (i.e. the higher loss section of the overall pattern), however they were also observed in thinner (lower loss) sections of the pattern as well. Pearce[4] observed that most patterns that had changed could be returned to their original condition by thermal annealing in high vacuum, as shown in Fig. 5, and suggested that the films were being modified over time rather than being removed (for example by sputtering). Note that the amount of loss on the rod as plotted in Fig. 5 is inverted from the traditional sense (e.g. Fig. 4). Although somewhat confusing, this is the standard way of plotting attenuator rod patterns, as they measure the amount of RF transmitted through the pattern rather than the amount of RF absorbed by the pattern.

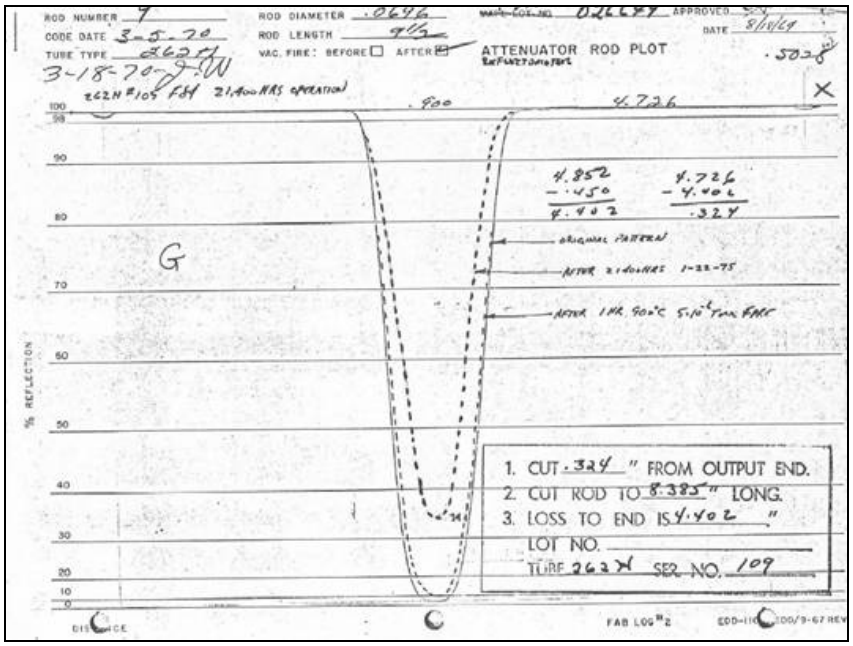

Fig. 5. Earliest documented record of attenuator pattern change and recovery mechanism, March 1970. Support rod was removed from TWT showing gain growth. Attenuation pattern reduction after 21,400 hours of operation and recovery of pattern after thermal processing in-vacuum at 900 C. From Pearce, Ref. 4.

Wachi[5] provided the first hypothetical model of attenuator degradation, suggesting surface interactions (chemisorbtion) between carbon and residual hydrogen and/or oxygen as the primary cause of resistance changes with secondary processes such as ion- or electron-bombardment-induced changes also being possible. Noting that there were often large variations in the time required for gain changes to occur, he further developed his hypothesis to include rate effects, suggesting that the initial hydrogen and oxygen content of the internal TWT surfaces was the rate controlling mechanism. To address non-recoverable resistance changes, Wachi noted that although low energy electron bombardment (from the TWT electron beam) could not remove carbon directly, electron induced desorbtion of carbon-oxygen molecules could overcome this energy requirement.

Pearce[6] later performed detailed experiments on attenuator film stability, subjecting films to low-energy plasmas of typical TWT residual gas species. Pearce found, in decreasing order of reactivity, that oxygen, followed by carbon dioxide, hydrogen, water and nitrogen would result in non-recoverable changes in film resistance. Methane and carbon monoxide plasmas were indicated as not reactive. Pearce did not observe recovery of the film resistance by thermal annealing, contrary to what he had seen in attenuators removed from actual TWTs. Failure to replicate this key TWT behavior (reversibility), was explained as likely due to too high of ion energy sputtering the carbon film. Pearce investigated all common attenuator substrates, and found no correlation between resistance change and substrate material.

Goebel[7] proposed that hydrogen ion bombardment of the carbon film was responsible for gain change, based on the results from plasma-edge studies by Wampler[8]. Wampler noticed that carbon resistance probes will change value when immersed in an energetic hydrogen flux, and concluded that energetic particle bombardment caused displacement damage to the carbon lattice, modifying the resistivity. Goebel further proposed that gain change rates were proportional to TWT cleanliness, with a larger initial rate proportional to an exponential decay of TWT pressure, followed by a lower constant rate as the internal surfaces of the TWT clean up and the pressure stabilizes to a constant "background" level[9]. The model for gain change over time from Goebel's theory is:

$$G = \beta\left[1 - e^{-t/\tau} + \frac{P_b t}{P_0 \tau}\right] + G_0,$$

where G is the gain of the TWT, β is a TWT geometry/material factor, t is operational time, τ is the TWT pumping time constant, P_b is the background pressure of the TWT, P_0 is the initial pressure of the TWT, and G_0 is the initial gain of the TWT. The $(1-e^{-t/t})$ term is a transient term which dies away with time, while the $P_b t/P_0 \tau$ term allows for a linear increase in gain throughout the operational life of the TWT. This theory has since been modified to have an exponential time constant multiplying the linear term (different from the pumping time constant) which allows the linear term to die out over time due to saturating damage of the attenuator pattern. This addition to the theory was found to better match measured long-term gain growth data.

Although both Wachi's and Goebel's models are well founded and appear to adequately predict gain change caused by degradation of the attenuator film, the models are quite different physically. Neither author presented direct evidence supporting their theory other than matching the temporal evolution of observed TWT gain changes, nor did they present evidence supporting both reversible and irreversible resistance modification seen in rods removed from TWTs.

Chemistry of Carbon Attenuator Films

Carbon has two well known allotropes, diamond and graphite, with diamond consisting of sp3 hybridized carbon-carbon bonds whereas graphite consists of sp2 hybrids. Hybridization manifests each form with entirely different physical properties, with diamond being hard, non-conductive (electrically) and optically transparent, contrasted to graphite which is soft, electrically conductive and opaque.

Sp3 hybridization (diamond) occurs when a 2s electron is promoted to a 2p shell. This results in a heavily distorted electron orbit that promotes strong covalent bonds, no free electrons, and results in an insulator. In sp2 hybridization (graphite), one 2s electron is mixed with two 2p orbitals leaving the 6th electron unlocalized or free[10]. This bonding configuration is responsible for the planar structure of graphite and its good electrical conductivity.

Electron diffraction patterns (Figs. 6, 7) indicate that the thin films applied to the attenuator rods consist of graphite (sp2) in a polycrystalline or amorphous state. The films appear similar to glassy carbon, which consists of carbon chains, analogous to polymeric chains (Fig 8). Some percentage of sp3 hybridized carbon should also be present however the exact sp2 to sp3 ratio in these films is unknown[10].

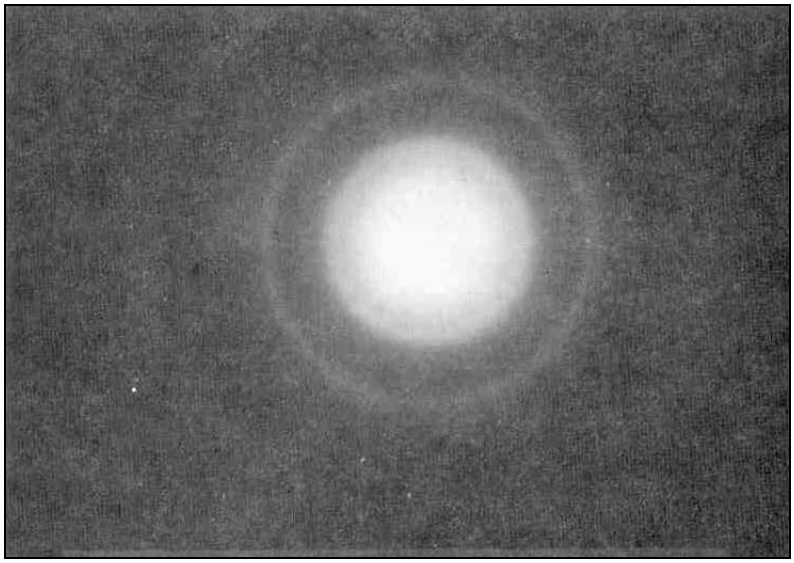

Fig. 6. Diffraction pattern (reference) for glassy carbon. From Wachi, Ref. 5.

All TWT attenuators and the experimental attenuator films used in this study were deposited by thermal decomposition of a precursor molecule (typically methane), however plasma chemical vapor deposition (PCVD) and sputter coating are other common methods used to deposit carbon films. Amorphous films can exhibit a variety of characteristics depending on the precursor molecule, deposition technique, deposition energy, etc[11]. Significant hydrogen (>30%) can also be incorporated into the films, as well as impurities that can act like electronic dopants used in semiconductors.

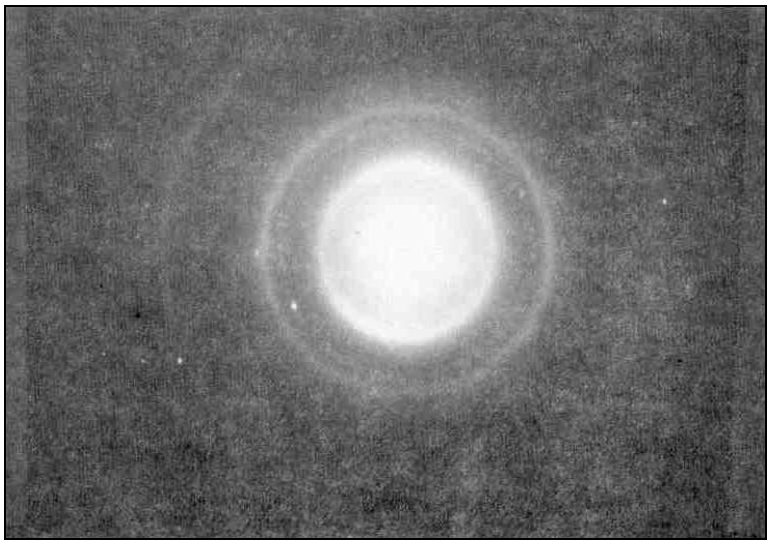

Fig. 7. Diffraction pattern for carbon attenuator film on beryllium oxide substrate. From Wachi, Ref. 5

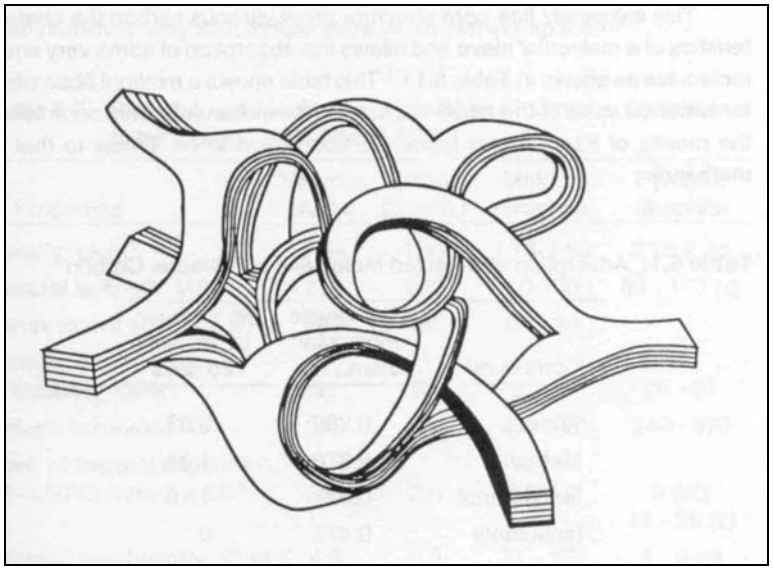

Fig. 8. Proposed structure of glassy carbon. The polymeric structure has no long-range order, and is thought to include both sp2 and sp3 bonding. Adapted from H.O. Pierson, Ref. 10.

It has been shown that significant amounts of hydrogen can be liberated from carbon films at temperatures in the range of 350 to 500 C^{12}. Thermal processing removes the hydrogen incorporated in the film and favors sp2 over sp3 hybridized carbon (hydrogen bonds preferentially to sp3 hybridized carbon). Thermal processing is often referred to as graphitization (Fig 9).

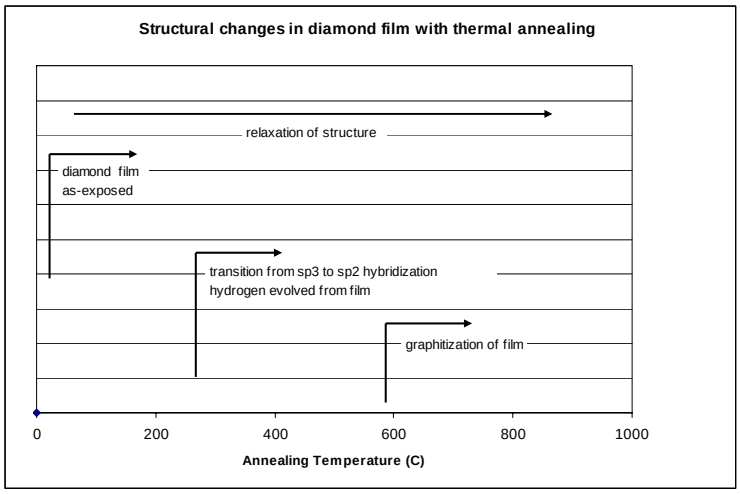

Fig. 9. Structural changes in diamond film as a function of annealing temperature. Note sp3 to sp2 transition beginning at approximately 300 C. As-exposed samples at 25 C. Adapted from Yamakazi, Ref. 12.

TWT attenuator films typically receive a vacuum annealing at 700-1000 C following carbon coating. This thermal processing is done to insure that the rods are clean and free from incomplete decomposition products prior to being built into a vacuum tube. This thermal processing (in principal) would tend to increase the graphitic nature and lower the resistivity of the film. As expected, vacuum processing of as-deposited attenuator films does in fact increase the loss of the attenuator pattern. (Fig.10)

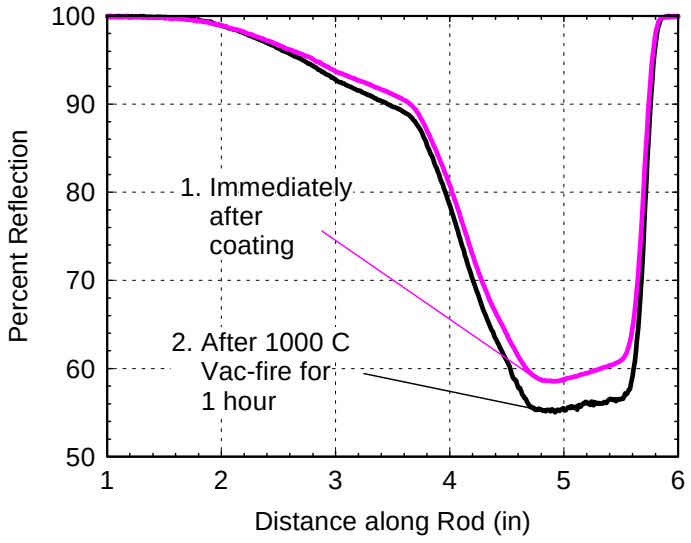

Fig. 10. Increase in attenuator pattern loss (decreased film resistivity) following thermal annealing at 1000 C.

Optical Properties

Attenuator coatings removed from TWTs with gain change (growth) often appear visually lighter in appearance, and in certain cases the thinner sections of the pattern appear to have been removed altogether. This may be explained by the optical bandgap of the film, which can be correlated with the sp2/sp3 ratio, ion impact, annealing temperature, etc. Films with higher hydrogen content have a lower optical density[13]. A change in optical density would be consistent for films that appear lighter or missing (after ion bombardment) yet can be recovered by thermal annealing.

Energetic Particle Damage to Attenuator Films

Energetic particles (typically ions) bombarding materials can alter material properties in numerous ways, and at sufficient energy can physically remove the material by sputtering. Depending on the dynamics of impact, ions can reflect or implant. Impacting particles increase the energy in the substrate and can result in grain modification, dislocations, atom substitution, etc.[14] Numerous impacts may occur before the impacting ion energy is expended, resulting in a damage tree or cascade. Due to their mass, electron collisions are not normally damaging at TWT beam energies unless a large amount of intercepted electron current becomes thermally destructive.

Binary Collision Simulations

Monte Carlo simulations of ion-matter interactions can be used to evaluate energetic particle-target interactions. These codes typically treat the target and impacting ion as a classical elastic collision, with momentum exchange being maximized if the particles are of similar mass. TRIM[15], a well known ion range code calculates the ion trajectories of a collision and reports displacement, sputtering, ion range (implant depth), and several other parameters.

Wampler used TRIM to calculate the damage cascades of hydrogen (and deuterium) incident on graphite and concluded that displacement damage was the cause of resistance changes. In TRIM, a displacement is defined as a collision that causes a vacancy and/or replacement collision.

Depending on incident particle energy, just target atoms may be ejected (displacements) or both the target and the incident ion may be ejected (vacancy). Under certain energy circumstances a replacement collision can occur. In a replacement collision the incident ion replaces a *like* stopped ion, netting no new displacements. Replacement collisions are likely the saturation or limiting mechanism of gain change.

Simulating Ion Collisions onto a TWT Attenuator

Low energy ($\leq$ 150 eV) ion bombardment was suggested previously as a likely mechanism for the TWT gain change observed during initial burn-in and through end of life[7]. In the TWT vacuum environment, there exists a low background pressure of

residual gasses either not removed completely during bake-out, or evolved from within the tube during life. After a normal 500 C vacuum bakeout, the primary residual gas in a TWT will be hydrogen, and will make up the majority of the TWTs residual pressure. This equilibrium partial pressure occurs due to (atomic) hydrogen in the metals that make up the TWT and any hydrogen which diffuses through these materials. If this hydrogen is ionized by the TWT's high-energy (several kV) electron beam, there exists the opportunity for ion bombardment upon the carbon loss pattern.

As the loss pattern is damaged, the resistivity of the carbon film and hence the gain of the TWT may change. Testing this assumption without having to wait thousands of operating hours (as required in a TWT) necessitated an accelerated life test apparatus for rapidly performing damage experiments on the loss patterns while simulating the environment of a TWT. Such an apparatus would allow rapid experiments to help understand the physics of the damage process. Such a rapid method of assessing attenuator stability would then enable designers to quickly produce and evaluate more resilient loss patterns, eliminating or mediating TWT gain change over life.

Production of Attenuator Carbon Films

Sample carbon films were prepared on beryllium oxide (BeO) rods by pyrolytic deposition of methane, with pattern depth (film thickness) varying as a function of position along the rod. Methane gas is injected into a furnace operating at 1000-1200 C which thermally liberates (cracks) much of the hydrogen, leaving carbon as the primary species in the deposition process. The furnace includes a small aperture through which the methane fragments flow toward the rod and are deposited. Stepper motors feed the rod past the aperture at a controlled rate, such that the exposure time at any point along the rod is known. A subsequent vacuum-firing of the film (550-900C) at pressure $\leq 1x10^{-7}$ Torr is performed, which, as described by Ulbricht[18], liberates additional hydrogen and oxygen residing in the film, while simultaneously annealing the carbon to form a patchwork of graphite crystals. As shown previously (Fig. 10), thermally annealed films generally showed higher RF loss (lower film resistivity) than the as-deposited carbon film.

Hydrogen Ion Production

A commercial Kaufman[16]-style plasma ion source was modified similarly to that as described by Sharp[17] to produce low-energy hydrogen ions. Normally employing argon for sputter-etch applications, Kaufman sources produce ions by electron impact which are removed from the plasma and accelerated across a closely spaced multi-aperture grid set. Typically, ion energies in the 1-2 keV range are generated, however these ions are much too energetic for evaluation of the 5 eV damage threshold suggested by Wampler.

Kaufman sources use magnetic cusps to improve ionization efficiency, allowing low pressure operation. A pressure of $1x10^{-4}$ Torr was used in all cases. During operation, the electron impact potential was set at 60 volts for efficient ion production, while screen and

extraction grid potentials were set to minimize ion energy. Ion energies of approximately 16 eV could be stably produced using argon; however source stability at ion energies below 60 eV was not possible with hydrogen, requiring additional energy filtering.

Kaufman sources typically include a tungsten filament hot-cathode electron source for charge neutralization, however to avoid thermal deposition of tungsten onto the attenuator film this source was not used.

Verification of Attenuator Resistance Profiles

The gain characteristics of a TWT are carefully tuned through the use of controlled loss patterns. To verify a pattern is correct, loss is measured by pushing the rod through an aperture in shorting-plane terminated rectangular waveguide at a controlled rate, wherein it is exposed to microwave energy (Fig. 11). The rod "loss" pattern absorbs the microwave energy, modifying the standing wave amplitude. Sections of attenuator rod without a carbon coating result in 100% wave reflection (no loss), whereas the thick or "deep" loss sections result in significant attenuation. A loss "pattern" is generated by plotting loss as a function of distance along the rod, as shown previously in Fig. 5.

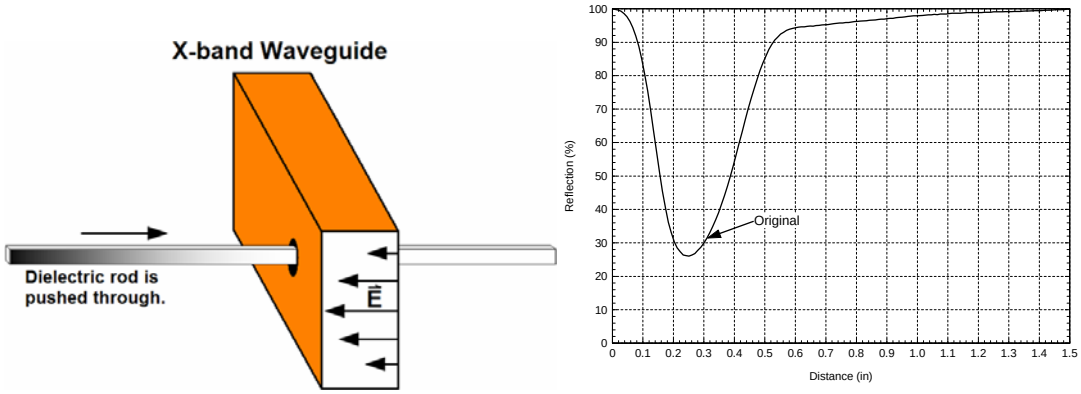

Fig. 11. Rod plotting system.

Ion Bombardment of Sample Loss Patterns

Coated rods were exposed to hydrogen ion bombardment at low energies as described by Goebel. To accomplish this, an ion source (Ion Tech MPS 3000 FC) was installed in a high vacuum chamber and configured for hydrogen plasma output (Fig 12) . The source is capable of producing ~ 250 mA of ion current in a 5 cm diameter column, with energies ranging from approximately 50 eV to 1keV. The source produces an ion fluence that simulates gain growth in a matter of seconds or minutes (a process that normally takes years in a TWT), and the extracted beam is energetically chromatic with an energy distribution of 30 eV FWHM, as shown in Fig. 13. This beam energy spread made precise damage threshold measurements impossible, but did generate resistance changes identical to that seen in TWTs (Fig 14).

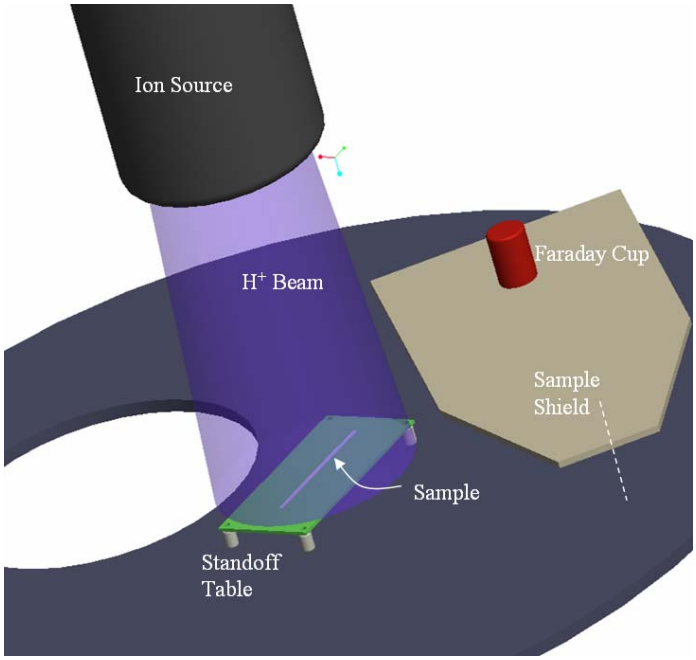

Fig 12. Ion bombardment system with chromatic energy distribution (without energy filter). Ion energy control is accomplished by applying a bias voltage to the sample table. Faraday cup and sample shield allow ion beam to be characterized and ion source to stabilize before bombardment of sample.

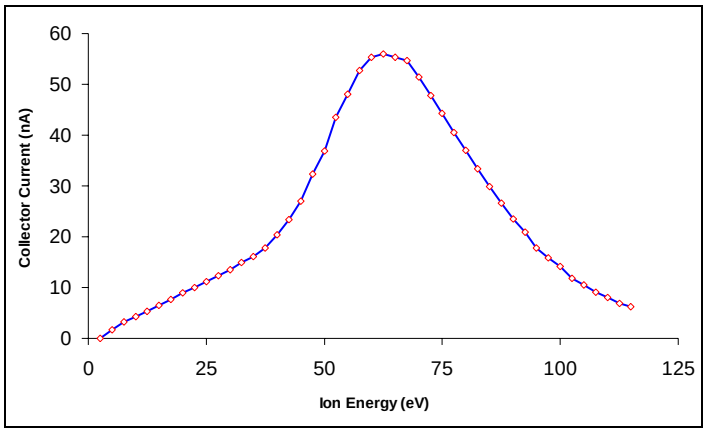

Fig. 13. Gaussian energy distribution of "chromatic" hydrogen ion beam generated by Kaufman ion source. The peak energy here is 60 eV, with a FWHM spread of approximately 30 eV.

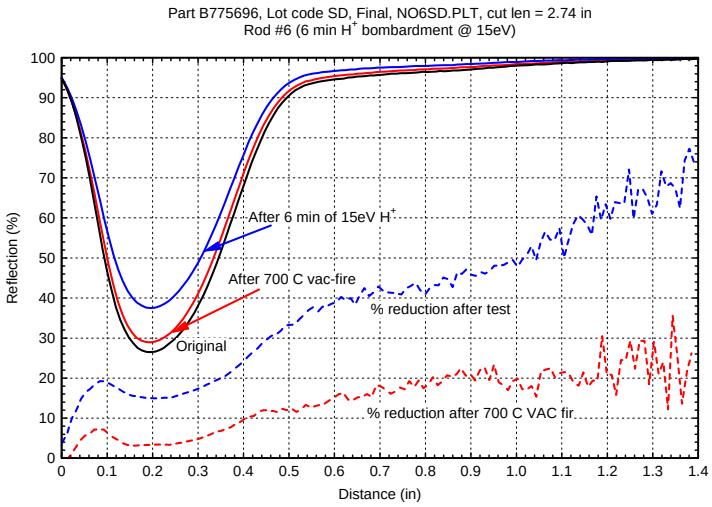

Fig. 14. Reduction in attenuator pattern loss from original (as-deposited) film, and pattern reduction caused by 15 eV hydrogen ion bombardment. Also shown is pattern recovery following thermal annealing at 700 C in vacuum. The dashed lines are the calculated percent reduction in reflection after the various processes.

Velocity Filtering of Ion Energy

Initial rod data was taken under the chromatic beam as previously discussed, with the sample reverse-biased to generate the desired impact energy. The effect of the beam energy spread was to limit the minimum energy to approximately 50 eV for these experiments, which is too high to investigate damage thresholds.

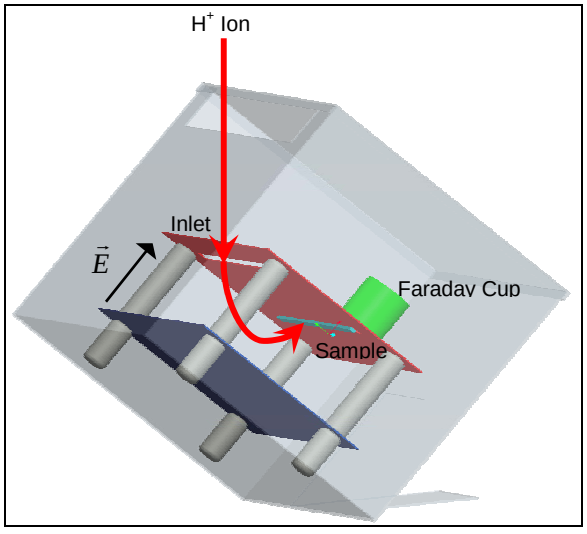

Fig. 15. Electrostatic energy filter with 45 degree beam entrance and in-situ Faraday cup. Ion energy is selected by varying the plate potential. Neutral atoms are collected on the lower plate, and do not impact test sample.

To produce a better quality, monochromatic beam, a planar mirror analyzer was developed similar to that described by Hofer[19] and shown in Fig. 15.

The dispersion characteristics of the filter allow energy selection (resolution) within approximately 5 eV across a spectrum of 1 keV, as shown in Fig. 16. The filter also excludes neutral atoms by geometrically shielding the sample. Rods to be tested were placed in line with the monochromatic beam while the current was monitored with an in-situ Faraday cup.

After ion bombardment, the loss pattern was remeasured by another scan through the waveguide system, allowing a direct comparison between the ion-exposed and the original patterns. To evaluate pattern recovery, rods then received a post-ion bombardment vacuum firing, followed by a third waveguide scan of the pattern.

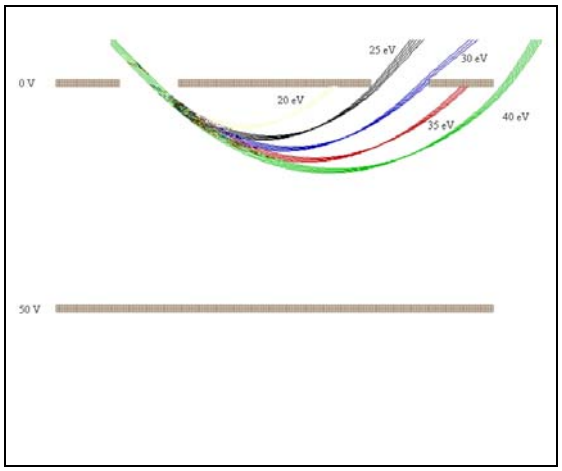

Fig. 16. Ion orbits in the electrostatic energy filter indicating an energy dispersion of approximately 5 eV. Ions enter the aperture at 45 degree incident angle.

The ion bombardment system with energy filter allows well defined ion beams to be generated and applied to test loss patterns. Following the beam characterization, various experiments were performed including evaluating modifications to the deposition process, evaluation a protective coating of quartz, modifications to the thermal processing, etc. As with the chromatic beam system, the instrument maintained the high fluence that allowed evaluation in minutes or hours process changes that might require thousands of operating hours in a TWT.

Results of the ion bombardment experiments

Initial ion bombardment experiments confirmed the hydrogen ion bombardment apparatus described above could reproduce the loss pattern changes seen in TWTs that exhibit gain change. Fig. 17 compares the loss plot from a rod extracted from a TWT which exhibited significant gain change over life to the loss plot from a rod damaged by

15 eV hydrogen ions for 1 hour under a chromatic beam in the ion-bombardment chamber.

Three major pattern characteristics are normally observed in a life test rod (i.e. a rod removed from a TWT which underwent gain growth) which can also seen in an experimental rod treated by the ion system. 1) After the damage period, the original loss pattern (black curves in Fig. 17) shifts upward (less loss or higher resistance) throughout the pattern. This is most noticeable in the deep (thick carbon coating) region where the loss increased approximately 15 to 20% (blue curves in Fig. 17). 2) After an annealing vac-fire of 700 C (post ion bombardment), each loss pattern returns to within 1 to 5 % of its original value (red curves in Fig. 17).

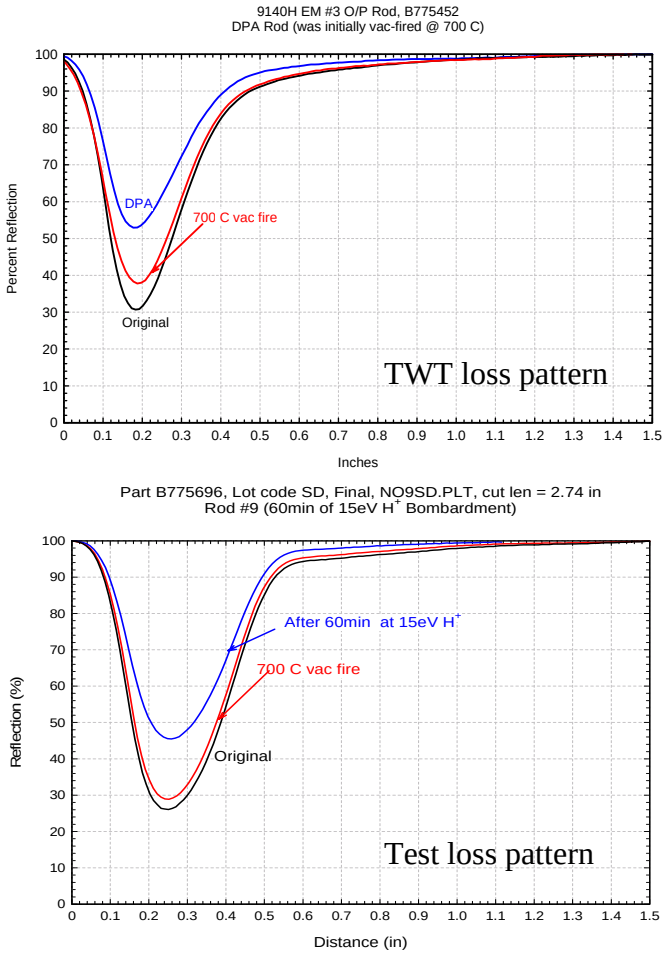

Fig. 17. Comparison of attenuator damage produced by actual operation in a TWT (upper plot) vs. that experimentally created by hydrogen ion bombardment (lower plot).

As suggested by Goebel, pattern recovery is likely due to recoverable bond structure damage caused by low energy ion bombardment. 3) Neither loss pattern returns

completely to its original state, suggesting an additional permanent damage process which still results in some gain growth, but to much less of an extent. These experiments indicate that the ion bombardment system quickly generated changes in loss patterns identical to that seen during TWT operation.

Reducing the effects of ion impact on attenuation patterns

Several different experiments were performed to investigate the possibility of inhibiting loss pattern damage. As previously suggested, lowering the original rod vacuum firing temperature may reduce loss pattern damage by leaving more residual bonded hydrogen in the film. Preliminary results suggest this to be the case, at least for the deep section of the pattern. As was shown in Fig. 17, attenuation patterns that were initially vacuum annealed at 700 C (after carbon deposition and before ion bombardment) exhibit nearly a 20% increase in RF reflection (decreased film resistance) in the deep section after being exposed to 15 eV hydrogen ions, whereas patterns initially annealed at 550 C (a typical TWT bakeout temperature) before being exposed to hydrogen ions change by only 1-2 %.

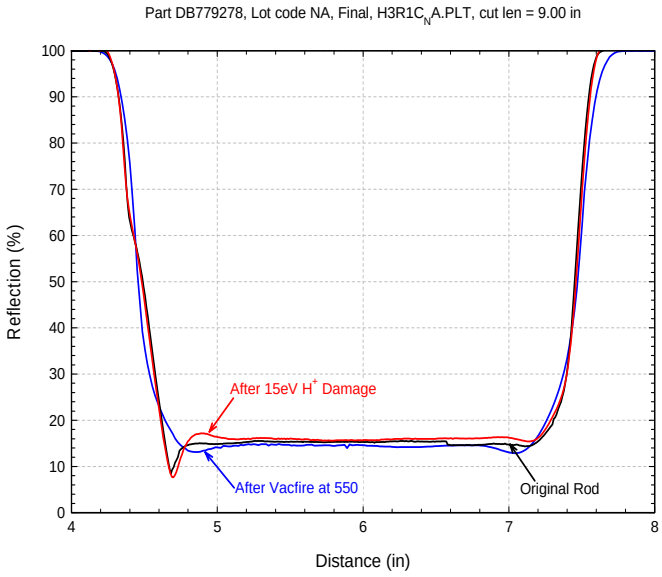

Fig. 18. Damage due to hydrogen bombardment in the deep-loss section of the attenuator pattern for 550 C vacuum fired film. Lower firing temperature (i.e. 550 C instead of 700 or 900 C) decreases the film sensitivity to ion damage. Shallow loss patterns did not show a similar response, possibly due to the energy spread of the ion beam (see Fig. 13).

An example of low temperature annealing is shown in Fig. 18; a modified loss pattern (deep only) rod was vacuum fired at 550 C then exposed to 15eV ions for 60 minutes and showed little resulting change in its loss pattern. Unfortunately vacuum-firing the rod patterns at a lower temperature before exposing them to hydrogen ions ("pre-vacuum-firing") does not seem to keep the low loss (shallow) regions of the pattern from changing. Moreover, the damage to the shallow loss regions seems irreversible and equal to the non-recoverable amount referred to in Fig. 17. This phenomenon was observed in

the tail region of films pre-vac-fired at either 550 or 700 C. These results were preformed under both the chromatic energy source and the filtered (monochromatic) energy source. Under the chromatic energy source, carbon sputtering due to the high energy beam tail might explain the observed permanent damage, because using energy-filtered 15 eV ions resulted in substantial recovery following a subsequent vacuum firing (Fig. 19). That is, most of the damage from the 15 eV filtered ions was not permanent. It is critical to determine the affect of ion damage on low-loss regions of the pattern because TWT gain growth is most sensitive to this damage, as shown in Fig. 20.

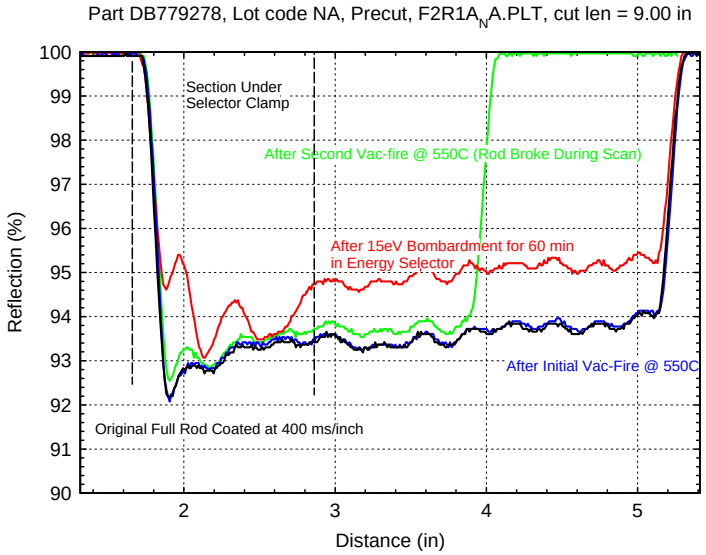

Fig.19. Recovery of shallow attenuation pattern region by vacuum firing at 550 C following 60 minute exposure to energy-filtered 15 eV hydrogen ion bombardment. This recovery is similar to that shown in Fig. 12.

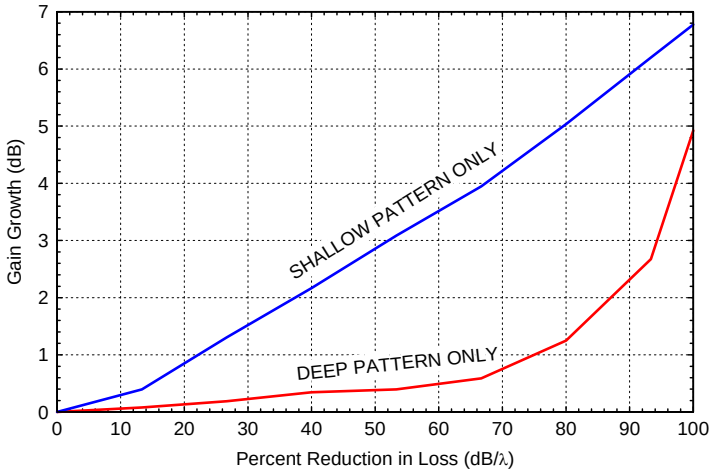

Fig. 20. Impact of loss pattern damage on TWT gain growth for a typical space TWT. The gain growth is much more sensitive to shallow pattern damage than to deep pattern damage.

Understanding how incident ion energy affects loss pattern damage is of much importance as demonstrated previously. Through the use of both a chromatic beam and the above described energy filter, data was taken at several different ion energies. Preliminary results from these experiments are shown in Fig. 21. In the deep region, the loss pattern damage goes up as a function of ion energy and then reaches an asymptote, in agreement with Wampler.[5] Again the shallow region does not exhibit the same trend, and is linear with respect to ion energy. Figure 21 does not indicate how much of the damage in each case is permanent and how much can be recovered by an annealing vacuum firing.

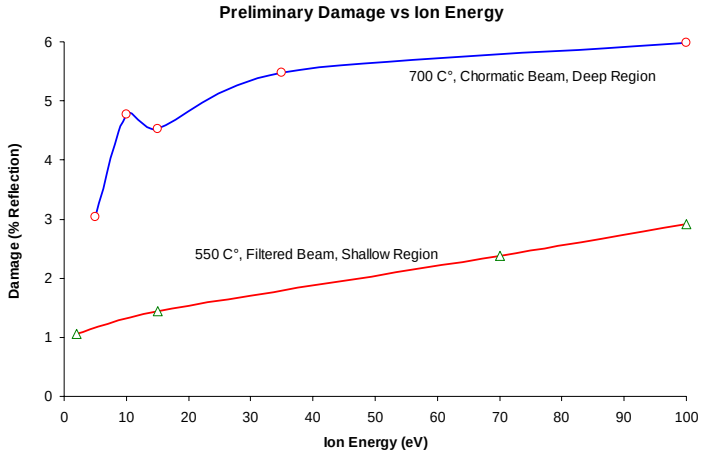

Fig. 21. Ion damage effects for two different attenuator film thicknesses. The red curve shows that shallow loss patterns have a linear relationship (damage) with ion energy, and the blue curve shows that deep loss patterns have an asymptotic behavior (as seen by Wampler).

Protective coatings to prevent ion damage

As suggested by Wampler, a thin insulating layer placed on top of a carbon resistive film may stop ions below the sputter threshold energy from reaching the loss pattern, thus eliminating modification of the carbon film. Goebel echoed this suggestion, mentioning that a protective coating might similarly protect the attenuator film, eliminating gain change.

To test the protective coating hypothesis, a standard attenuator rod was vacuum annealed at 700 C and then RF sputtered coated with 0.1 μm of quartz (SiO_2). The coated rod was then exposed to several different levels of ion energy, the results of which can be seen in Fig 22. The quartz coating modified the loss pattern, however this was expected and could be compensated for by modification of the original carbon film thickness profile.

The quartz protective coating appeared to completely protect the loss pattern from damage, even after several minutes of 1keV exposure (Fig. 22). Based on TRIM calculations, a 0.1 μm (1000 Å) layer is adequate to protect the carbon film (Fig. 23); however any ion collisions depositing enough energy into the quartz layer greater than surface binding energy of quartz, approximately 3.4 eV, would eventually remove the protective coating by sputtering. Loss of the protective coating can clearly be seen in Fig. 22, where the light blue curve shows the measured loss pattern after 60 minutes of 1 keV hydrogen ion exposure. TRIM calculations indicate hydrogen ions with energies greater than 70 eV may start to sputter the protective coating (Fig. 24). Note that these calculations are for atomic hydrogen ions (protons).

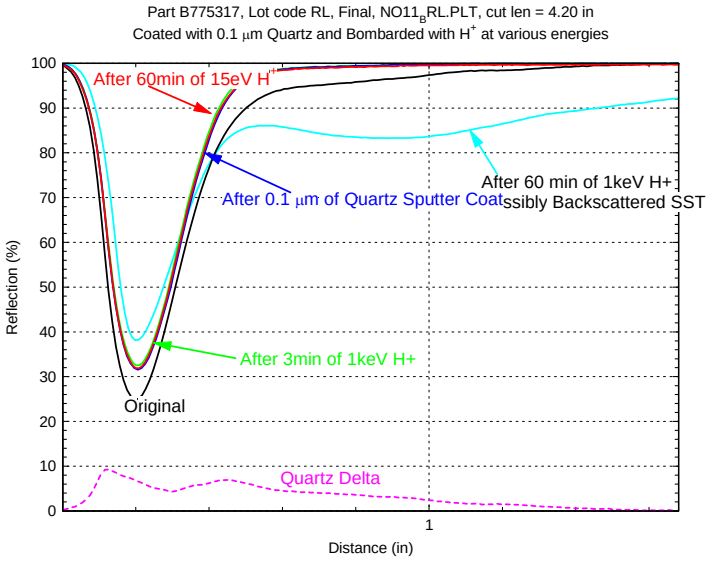

Fig. 22. Performance of quartz protective coating after exposure to hydrogen ions of varying energies and durations. Pattern stability indicates no modification (complete protection) of resistive film from ion impact. Removal of protective film by higher energy (1 keV) ions also evident (light blue curve).

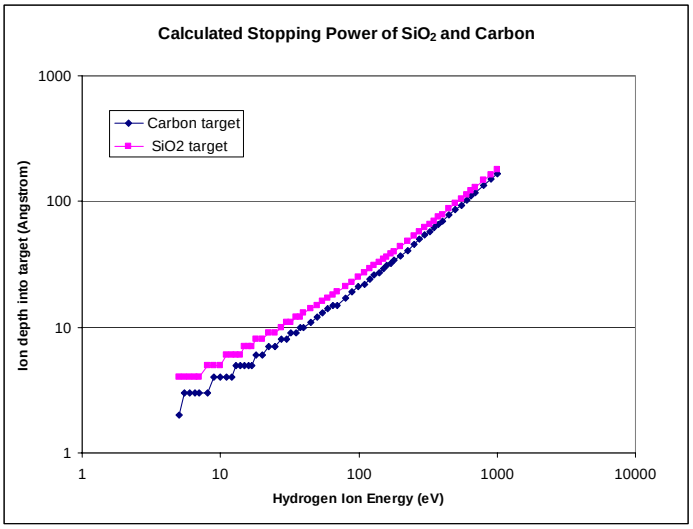

Fig. 23. The stopping power of SiO_2 to hydrogen ion impact indicates that a 0.1 μm (1000 Å) protective layer would adequately shield the attenuator film; however, long term protection would depend on the fraction of target ions that can deposit sufficient collision energy in the film above the SiO_2 surface binding energy of 3.4 eV, where sputtering of the coating will occur.

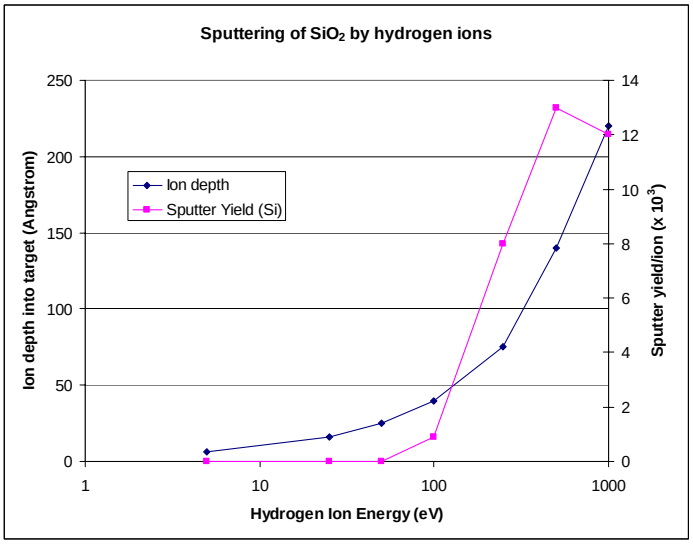

Fig. 24. Sputter yield for atomic hydrogen ions impacting quartz substrate. The range of the ions is less than 0.02 μm. Ion energies above 70 eV may cause SiO_2 sputtering, eventually depleting the protective coating.

Discussion

It has been shown that the change in loss patterns seen in TWTs experiencing gain growth can be quickly reproduced in a laboratory setting by bombarding the attenuator

pattern with hydrogen ions. This behavior is in agreement with the theory suggested by Goebel, et. al. Based on examination of rods extracted from TWTs which have exhibited gain growth, most of the loss pattern damage appears to be from low energy ion bombardment and is reversible by thermal annealing in vacuum. Patterns that were experimentally damaged also contain a small percentage of damage that is non-recoverable, again identical to that seen in rods recovered from operated TWTs that exhibited gain change.

Diffraction patterns indicate that the attenuator patterns are isotropic, consisting of randomly oriented microcrystallines of graphite. This amorphous structure appears to have characteristics of polymer-like amorphous carbon, incorporating significant hydrogen and having both diamond-like and graphite-like film characteristics. Ion bombardment appears to increase the sp3 or "diamond-like" nature of the film, increasing the film resistivity and reducing the optical density.

Investigation and modification of the film structure was beyond the scope of this project, however it may be advantageous to incorporate additional hydrogen in the film by modifying the precursor molecule, for example using acetylene instead of methane has been shown to increase the hydrogen evolution temperature several hundred degrees.[20] We have seen evidence that maintaining hydrogen in the film by simply reducing the original vacuum-firing temperature to that of tube bakeout can eliminate some of the ion damage, particularly in the deep-loss patterns, but this may or may not be sufficient to reduce gain change to acceptable levels.

As indicated by Wampler, adding a protective over-layer to the film can protect from ion implantation and stabilize the film resistance. In our investigations, both reversible and non-reversible film damage was eliminated by a thin layer of SiO_2. Oddly, adding quartz to a TWT is (from a materials point of view) returning to earlier times when the entire TWT vacuum envelope was quartz "glass". Other protective coatings based on oxides such as Al_2O_3 (alumina) may provide similar ion protection without adding additional "new" materials into the vacuum envelope (alumina is used as a ceramic voltage stand-off material in both the gun and collector of most TWTs).

Acknowledgment

The authors would like to thank Dr. Robert Barker, AFOSR for supporting this work, M. Richardson for providing the dielectric coatings, C. Pearce, and D. Goebel, for their many helpful comments and suggestions. This work supported by the Air Force Office of Scientific Research under contract FA9550-05-C-0173.

1. A.S. Gilmour, *Principals of Microwave Tubes,* Artech House, 1994.

2. L. R. Falce, “Improved techniques for producing pyrolytic graphite attenuator films for microwave tubes”, presented at the Microwave Power Tube Conference, Monterey, CA, 1966.

3. B. Behler (Private communication) 1970.

4. C. R. Pearce (Private communication) 1970.

5. F. M. Wachii, “Carbon-beryillia attenuator degradation phenomenon in a traveling-wave tube amplifier”, *Aerospace Corporation Report*, No. TOR-0074(4403-01), Vol. 1& 2, Nov. 1973.

6. C. R. Pearce, “Accelerated tests of attenuator stability, preliminary results of plasma exited gas reactions”, *Hughes Aircraft Company IR&D Report*, 1974.

7. D. M. Goebel, “Theory of long term gain growth in traveling wave tubes,” *IEEE Trans. Elec. Devices*, Vol. 47, No. 6, June 2000.

8. W. R. Wampler, “Plasma-edge studies using carbon resistance probes”, *J. Vac. Sci. Technol. A*, Vol. 3. No. 3, May/June 1985.

9. D. M. Goebel, “Gain increases through end of life in traveling wave tubes”, *IEEE Trans. Elec. Dev.*, Vol. 50 No. 4, April 2003.

10. H. O. Pierson, *Handbook of Carbon, Graphite, Diamond and Fullerenes*, Noyes, 1993.

11. S.R.P Silva, “*Microstructure in a-C*” from *Properties of Amorphous Carbon*, IEE, (UK), 2003.

12. Y. Yamazaki,”Structural change in diamond by hydrogen plasma treatment at room temperature”, *Diamond & Related Materials*, **14**, 2005.

13. W. R. Wampler, “Resistance probe for energetic particle dosimetry with applications to plasma edge studies”, *Appl. Phy. Lett.*, **41**(4) Aug. 1982.

14. R.U.A. Kahn, “Ion implantation of a-c”, from *Properties of Amorphous Carbon*, IEE (UK), 2003.

15. TRIM, the *Tr*ansport of *I*ons in *M*atter, www.srim.org.

16. H.R. Kaufman, *J. Vac. Sci. Technol.*, Vol. 15, 1978.

17. D. J. Sharp, “Applications of a Kaufman ion source to low energy ion erosion studies”, *J. Vac. Sci. Technol.*, Vol. 16. No. 6, 1979.

18. H. Ulbricht, “Thermal Desorption of Gases and Solvents from Graphite and Carbon Nanotube Surfaces,” *Carbon* **44**, 2931-2942 (2006).

19. R.R. Hofer, “Development of a 45-degree parallel-plate electrostatic energy analyzer for Hall thruster plume studies-preliminary results”, *Proc. 26th International Electric Propulsion Conference*, Kitakyushu, Japan, Oct. 1999.

20. J. Robertson, “*Hydrogen in a-C*” from *Properties of Amorphous Carbon*, IEE, (UK), 2003.